NON-ISOTHERMAL DECOMPOSITION OF N^1,N^4-DIBENZYLIDENEBENZENE-1,4-DIAMINE (DBBD) UNDER NITROGEN ATMOSPHERE

[1]S.M. Anuradha, [2]*M. Sekar, [3]V. Thanikachalam, [1]A. Kuraitheertha Kumaran, [1]G. Manikandan, [4]J. Venkatesan, [5]S. Arunadevi
[1]Assistant Professor, [2]Associate Professor and Head, [3]Professor, [4]Ph.D. Research Scholar, [5]Assistant Professor
[1]Department of Chemistry, Thiru Kolanjiappar Government Arts College, Virudhachalam 606 001, Tamil Nadu, India
[2,4]PG & Research Department of Chemistry, Government Arts College, C. Mutlur 608 102, Chidambaram, Tamil Nadu, India
[3]Department of Chemistry, Annamalai University, Annamalainagar 608 002, Tamil Nadu, India
[5]Department of Chemistry, Urumu Dhanalakshmi College, Tiruchirappalli 620 019, Tamil Nadu, India
[2]*E-mail: drmschemgac@gmail.com

ABSTRACT: Phenylamine Schiff base namely N^1,N^4-dibenzylidenebenzene-1,4-diamine (DBBD) has been synthesized from *p*-phenylenediamine, aldehyde and few drops of glacial acetic acid by condensation method and characterized by microanalysis, Fourier transform infrared (FT-IR) and NMR (^{1}H and ^{13}C) spectroscopic techniques. The thermal decomposition of DBBD was studied by thermogravimetry under nitrogen atmosphere at different heating rates of 10, 15 and 20 K min^{-1}. The decomposition process of DBBD is occurred in two steps as evidenced from thermogram. The kinetic parameters were calculated using model-free methods (Friedmann, Kissinger-Akahira-Sucrose (KAS) and Flynn-wall-Ozawa (FWO)) and model-fitting method [Coats-Redfern (CR)]. The calculated invariant kinetic parameters of DBBD are consistent with the average values obtained by Friedmann and KAS isoconversional method and each step of decomposition is followed different kinetic models. The first stage of thermal decomposition of DBBD was described by a P2 model and second stage described by a P3 model.

Keywords **– phenylamine Schiff bases, non-isothermal, invariant kinetic parameters.**

1. INTRODUCTION

Schiff bases and their derivatives are used in optical and electrochemical sensors, as well as in various chromatographic methods to enable detection of enhanced selectivity and sensitivity [1–3]. Among the organic reagents actually used Schiff bases posses excellent characteristics, structural similarity with natural biological substance relatively simple preparation procedures and the synthetic flexibility that enables design of suitable structural properties [4]. Schiff bases are widely applicable in analytical determination using condensation reactions of primary amines and carbonyl compounds in which the azomethine bond is formed (determination of compounds with an amino or carbonyl group) using complex forming reactions (determination of amines, carbonyl compounds and metal ions) or utilizing the variation in their spectroscopic characteristic following changes in pH and solvent [5]. Schiff base play important role in coordination chemistry as they easily form stable complexes with most transition metal ions [6]. Many biologically important Schiff bases have been reported in the literature possessing anti-microbial, anti-fungal, anti-inflammatory, anti-convulsant, anti-tumour and anti-HIV activities [7–10]. Another important role of Schiff base structure is in transamination [11]. Phenyl-amine based Schiff base act as a fluorescent chemosensor for the dual-channel detection of Hg^{2+} and Cu^{2+} with high selectivity and sensitivity [12]. Schiff's bases also used as anticancer and antiviral agents [13] and its metal complexes have been widely studied because they have industrial, anticancer herbicidal application [14], antitubercular activation [15] and chelating abilities which give it attached remarkable attention [16]. Schiff bases can participate in their inhibitor activity [17], anticarbonic anhydrase [18]. Literature survey reveals that no work has been reported on thermal decomposition of bis Schiff base under non-isothermal decomposition in the presence of nitrogen atmosphere. This prompted us to carry out the synthesis, spectral characterization and thermal studies of N^1,N^4-dibenzylidenebenzene-1,4-diamine (DBBD).

2. MATERIALS AND METHODS

2.1. Materials

Starting materials obtained from BDH chemicals of Analar grade 4,4′-phenylenediamine, sd-fine chemicals of Analar benzaldehyde were used without purification. Analytical grade solvents like ethanol, ethyl acetone hexane, dimethylsulfoxide (DMSO) and $CDCl_3$ were used as such without further purification.

2.2. Methods

Analytical thin layer chromatography (TLC) was performed on pre-coated plastic sheets of silica gel G/UV-254 of 0.2 mm thickness. Melting points of the synthesized compound was determined in open-glass capillaries on a Mettler FP51 apparatus and recorded in °C without correction. Elemental analyses were performed in EURO VECTOR EA 3000 at Central Leather Research Institute (CLRI), Chennai, India. FT-IR measurement was done on KBr pellets for solids using SHIMADZU-2010 Fourier transform Infra-Red (FT-IR) spectrophotometer (4000–400 cm^{-1}). The ^{1}H and ^{13}C NMR spectra were recorded in $CDCl_3$ using TMS as internal standard with Bruker 400 MHz and 100 MHz high resolution NMR spectrometer.

2.3. Thermal analysis

The simultaneous TG/DTA curves were obtained with the thermal analysis system model Perkin Elmer STA 6000, TEQP-II at CECRI, Alagappa University, Karaikudi, India. The TG analysis of DBBD was carried out under dynamic nitrogen atmosphere using Perkin Elmer Pyris TGA 6000 (0–200 mL min^{-1}) in an 180 µL ceramic pan with a sample at the heating rates of 10, 15 and 20 K min^{-1} from 35 to 700 °C.

In order to ensure the uniformity of temperature of the sample and good reproducibility, small amounts (10 mg) were taken. The sample temperature controlled by thermocouple, did not exhibit any systematic deviation from preset linear temperature programme. The kinetic parameters E_a and A were calculated using Microsoft Excel Software®.

2.4. Synthesis of title compound

The Schiff's base was obtained by refluxing equimolar quantities of benzaldehyde (0.02 mol), *p*-phenylenediamine (0.01 mL) and few drops of glacial acetic acid in 25 mL of ethanol are heated on a water bath for 6–8 h. After the completion of reaction, as monitored by TLC (ethylacetate-hexane (10.90%)), the resulting solution was cooled to room temperature, and they poured into crushed ice with constant stirring. The obtained precipitate was filtered and washed with cold water. The solid product was collected, dried using drying oven at 80 °C and recrystallized using ethanol. The yield of obtained product (Scheme 1) is 70%.

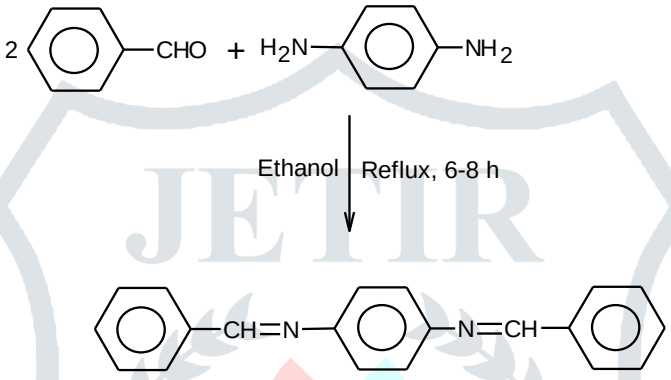

Scheme 1 Reaction pathway for the synthesis of DBBD

Pale brown colour solid. Calculated (Found), % for C: 84.21 (84.24); H: 5.96 (5.93); N: 9.82 (9.80). FT-IR (kBr, cm^{-1}): 3074 (CH), 2915 (aliphatic, C–H), 1605 (C–N), 3265 (N–H), 1513 (C=C) (Fig. S1). ^{1}H NMR ($CDCl_3$, δ, ppm): 8.51 (s, CH=N), 7.93 (d, C–H), 7.48 (t, C–H) (Fig. S2). ^{13}C NMR ($CDCl_3$, δ, ppm): 159 (CH=N), 149 (C–N), 136 (C–C), 131 (C–C) (Fig. S3).

2.5. Theoretical calculations

2.5.1. Model-free methods

Friedman method [19] is a differential method and is one of the first isoconversional method. The logarithmic form of Eq. 2 is given as

$$\beta\left[\frac{d\alpha}{dT}\right] = A\exp\left(-\frac{E}{RT}\right)f(\alpha) \qquad \ldots (1)$$

$$\ln\left[\beta\frac{d\alpha}{dT}\right] = \ln\left[A_\alpha f(\alpha)\right] - \frac{E_{a,\alpha}}{RT_\alpha} \qquad \ldots (2)$$

A plot of ln[βdα/dT] (or lnΔα/Δt) *versus* 1/T (Eq. 2), the activation energy E_a is obtained from the slope of the plot. The isoconversional integral methods suggested independently by Flynn and Wall [20] and Ozawa [21] uses Doyle's [22–24] approximation of p(x). This method is based on the Eq. (3),

$$\log\beta = \log\frac{AE_a}{Rg(\alpha)} - 2.315 - 0.4567\frac{E_a}{RT} \qquad \ldots (3)$$

For constant conversion of α, the left side of above equation against 1000/T, obtained from thermograms recorded at several heating rate, should be a straight line whose slope can be used to evaluate the apparent activation energy for a different level of conversion and Kissinger-Akahira-Sunose (KAS) equation [25,26] (Eq. 4) is

$$\ln\left[\frac{\beta}{T^2}\right] = \ln\frac{AR}{E_a g(\alpha)} - \frac{E_a}{RT} \qquad \ldots (4)$$

Thus for α = constant, the plot of ln (β/T^2) *versus* (I/T) should be a straight line, apparent activation energy obtained from the slope of plot.

2.5.2. Model-fitting method

Coats-Redfern method [27], which has been successfully used for studying the kinetics of dehydration and decomposition of different solid substances [27,28]. The kinetic parameters can be derived from modified Coasts-Redfern (Eq. 5),

$$\ln\left[\frac{g(\alpha)}{T^2}\right] = \ln\left[\frac{AR}{\beta E_a}\left(1-\left(\frac{2RT\exp}{E_a}\right)\right)\right] - \frac{E_a}{RT}$$

$$\cong \ln\left[\frac{AR}{\beta E_a}\right] - \left(\frac{E_a}{RT}\right) \quad \ldots (5)$$

Where g(α) is an integral form of the conversion function, the expression of which depends on the kinetic model of the occurring. If the correct g(α) function is used, a plot of ln [g(α)/T^2] against l/T gives a straight line, from the slope and intercept of the plot to determine E_a and the pre-exponential factor (A).

2.5.3. Invariant kinetic parameters (IKP) method

The invariant kinetic parameters method was applied to the data calculated for the different heating rates. Criado and Morales [29] observed, that almost any α = α(T) or (dα/dt) = (dα/dt) (T) experimental curve may be correctly described by several conversion functions. Further, the values of the activation energy obtained for various f(α) for single non-isothermal curve are correlated through the compensation effect.

$$\ln A_{inv} = a_\beta + b_\beta E_{inv} \quad \ldots (6)$$

The above Eq. 6 represents a linear relationship between ln A_{inv} and E_{inv} [30] any increase in the magnitude of one parameters is offset, or compensated, by appropriate increase of the other. Plotting ln A_{inv} *versus* E_{inv} for different heating rates, the compensation effect parameters a_β and b_β were obtained from the intercept and slope of this plot. These parameters follow an Eq. 7

$$a_\beta = \ln A_{inv} - b_\beta E_{inv} \quad \ldots (7)$$

The plot of a_β versus b_β, gives true values of E_{inv} and ln A_{inv} [31] are obtained from the slope and intercepts of this plot.

2.5.4. Determination of pre-exponential (frequency) factor and decomposition kinetic model

Based on the apparent activation energy (E_a) and reaction (conversion) model [g(α)], the value of A can be calculated from Eq. 8, in accordance with dependence g(α) *versus* $E_a p(x)/R\beta$.

$$g(\alpha) = \frac{AE_a}{R\beta} p(x) \quad \ldots (8)$$

Where g(α) is the integral form of the reaction model and p(x) is the temperature integral, for $x = E_a/RT$, which does not have analytical solution. For calculating the value of A for the investigated decomposition process, the fourth rational expression of Senum and Yang [32] for p(x) function was used. From the plot of g(α) *versus* $E_a p(x)/R\beta$, frequency factor (a) can be determined from the slope of the plot.

2.5.5. Thermodynamic parameters

The kinetics parameters, energy of activation (E_a) and pre-exponential factor (A) are obtained from Kissinger single point [25,33,34] kinetic method using the Eq. 9.

$$\ln\left(\frac{\beta}{T_m^2}\right) = -\frac{E_a}{RT_m} + \ln\left(\frac{AR}{E_a}\right) \quad \ldots (9)$$

Where, T_m is temperature that corresponds to the maximum of dα/dT. This model-free kinetic method can be applied with a reasonable approximation without being limited to *n*-order kinetics [35], providing a single E_a value for each reaction step. For this reason, it is often defined as a Kissinger single point method. The reaction proceeds under conditions where thermal equilibrium is always maintained, then a plot ln (β/T_m^2) *versus* $1/T_m$ gives a straight line with a slope equal to $-E_a/R$.

Based on the values of activation energy and pre-exponential factor for the decomposition stage, thermodynamic parameters $\Delta S^{\#}$, $\Delta H^{\#}$ and $\Delta G^{\#}$ for the formation of activated complex from the reactant were calculated based on the following [35–37] equations:

$$A = \frac{e\chi k_B T_p}{h} \exp\left(\frac{\Delta S^{\neq}}{R}\right) \quad \ldots (10)$$

The change of entropy may be calculated according to the formula

$$\Delta S^{\neq} = R \ln \frac{Ah}{e\chi k_B T_p} \quad \ldots (11)$$

$$\Delta H^{\neq} = E_a - RT_p \quad \ldots (12)$$

Where, e = 2.7183 is the Neper number: χ = transition factor, which unity for monomolecular reaction; k_B = Boltzmann constant, 1.3807×10^{-23} J K^{-1}; h = Planck constant, 6.626×10^{-34} J s^{-1} and T_p = peak temperature of DTA curve.

The changes in enthalpy ($\Delta H^{\#}$) and Gibbs free energy ($\Delta G^{\#}$) for the activated complex formation from the reactant can be calculated using the well-known thermodynamic equation.

$$\Delta G^{\neq} = \Delta H^{\neq} - T_p \Delta S^{\neq} \quad \ldots (13)$$

3. RESULTS AND DISCUSSION

3.1. Non-isothermal TG analysis

The thermograms of DBBD recorded in a dynamic nitrogen atmosphere at different heating rates of 10, 15 and 20 K min^{-1} are presented in Fig. 1. DBBD decomposed into two steps and distinct endothermic peak. The thermal decomposition process of DBBD, first stage starts at 388 to 499 K and ends at 559 to 596 K with the mass loss of 32% (Cal. 33%) removal of benzylidene group and second stage starts at 568 to 590 K and ends at 625 to 644 K with the mass loss of 68% (Cal. 67%) removal of benzylidenebenzene group at different heating rates.

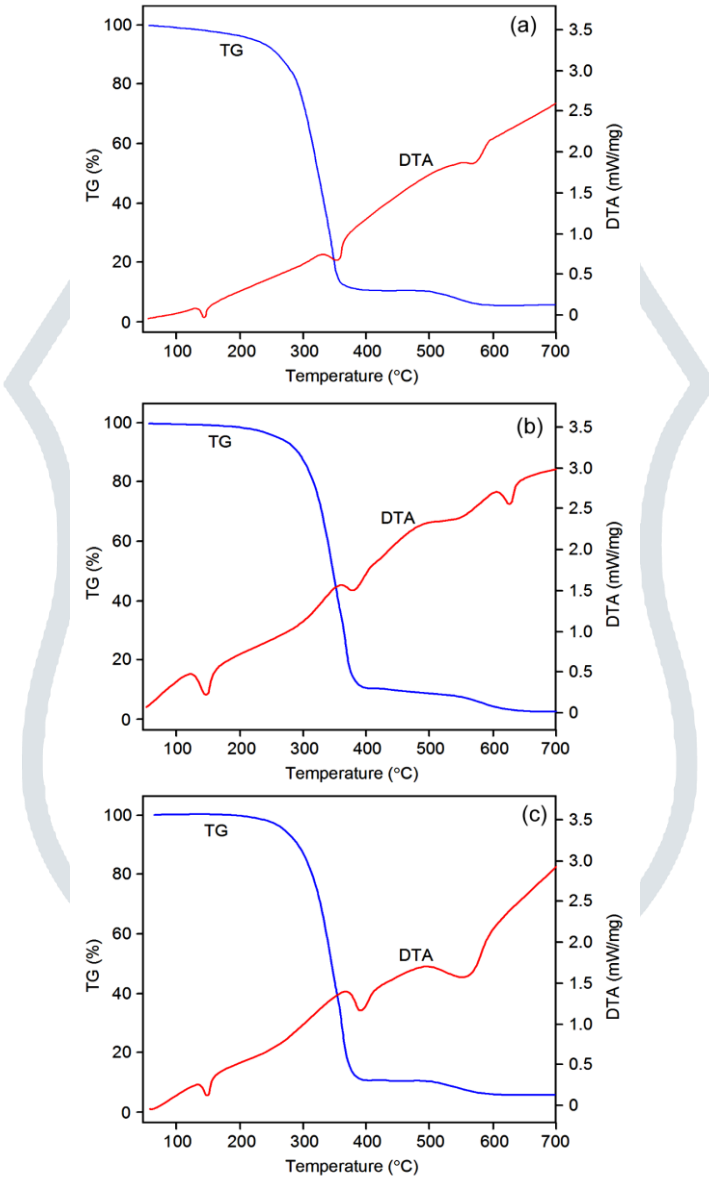

Fig. 1 TG-DTA curves of DBBD at a) 10, b) 15 and c) 20 K min^{-1} heating rates in nitrogen atmosphere

3.2. Model-free analysis

All results of non-isothermal TG analysis under nitrogen atmosphere and typical results of those under oxidizing atmospheres are shown Fig. 1. The obtained TG analysis data for the decomposition stages of DBBD were analyzed to determine the activation energy for a different level of conversion using Eq. 4. Slopes of the regression lines in the conversional plots for the each stage, which are shown in Figs. 2 and 3, were used to calculate the activation energy at each conversion degree. The non-isothermal decomposition kinetics of DBBD is first analyzed by model-free methods *viz.*, Flynn-Wall-Ozawa, Kissinger-Akahira-Sunose and Friedman (Tables S1 and S2) show that the variation of apparent activation energy E_a, as a function of extent of conversion α, for decomposition of DBBD. E_a values constant slightly in the conversion range of $0.05 \leq \alpha \leq 0.95$. It was pointed out [38] that when E_a changes with α, the Friedman, FWO and KAS isoconversional methods leads to different values of E_a. The applied isoconversional methods do not suggest a direct way for evaluating either the pre-exponential factor (A) or the analytical form of the reaction model $f(\alpha)$, for the investigated decomposition process of DBBD.

For the two stage decomposition of DBBD, the values of energy of activation corresponding to the different values of α for the decomposition process obtained by Friedman, KAS and FWO methods are used to determine kinetic parameter and are listed

in Tables S1 and S2 (Figs. S4 and S5). It is seen that E_a values depend upon the extent of conversion α. For stage I, the average value of E_a is 37.38 ± 11.531 kJ mol^{-1} (FWO) method. From Table S1 (Fig. S4), it is evident that the average activation energies obtained by Friedman method (52.55 ± 0.31 kJ mol^{-1}) is higher than FWO method. The average activation energy obtained by KAS method (30.36 ± 11.45 kJ mol^{-1}) is slightly lower than FWO method.

For stage II, the average value of E_a is 99.54 ± 10.53 kJ mol^{-1} (KAS method). From Table S2 (Fig. S5), it is evident that the average activation energies obtained by FWO method (104.28 ± 10.27 kJ mol^{-1}) is slightly higher than KAS method. The activation energies obtained by Friedman method (118.47 ± 0.26 kJ mol^{-1}) is higher than KAS method. From the E_a value we concluded that rate of decomposition in stage II is slower when compare to stage I.

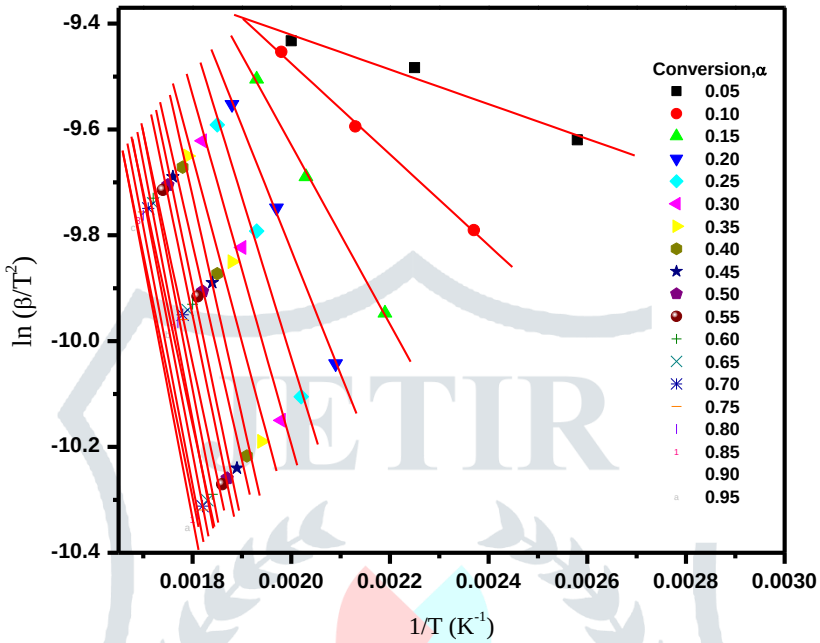

Fig. 2 Slopes of the regression lines in the isoconversional plots for DBBD (Stage I)

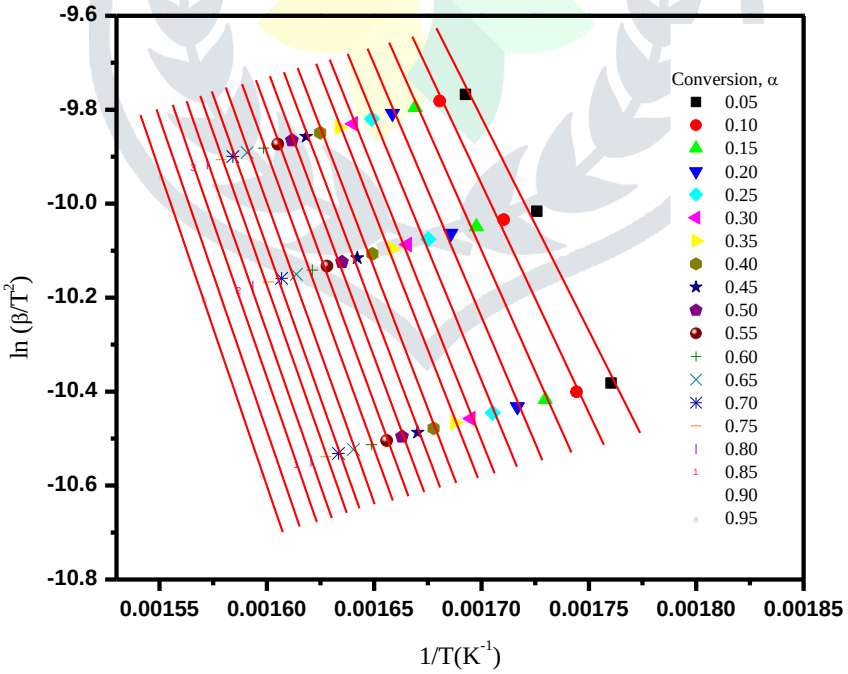

Fig. 3 Slopes of the regression lines in the isoconversional plots for DBBD (Stage II)

3.3. Model-fitting analysis

After the model-free analysis is performed, model-fitting can be done in the conversion region where apparent activation energy is approximately constant where a single model may fit. The non-isothermal kinetic data of DBBD at 0.05 ≤ α ≤ 0.95 where model-free analyses indicate approximately constant activation energy, were then fitted into each of the 15 models are listed in Tables S3–S8 for the applied method [33], Arrhenius parameters (E_a, ln A) for decomposition process, exhibit strong dependence on the reaction model chosen.

3.4. Invariant kinetic parameter (IKP) analysis

Criado and Morales [35] described that almost any $\alpha = \alpha(T)$ or $(d\alpha)/(T)$ experimental curve may be correctly described by several conversion function. The use of an integral of differential model fitting method leads to different values of the activation parameters. Although obtained with high accuracy the values change with different heating rates and among conversion functions. Lesnikovich and Levchik [39] suggested that correlating these values by the apparent compensation effect, $\ln A = a_\beta + b_\beta E_a$, one obtains the compensation effect parameters a_β and b_β, which strongly depend on the heating rates (β) as well as on the considered set of conversion functions. The invariant kinetic parameters method was applied to the data calculated for the heating rates 10, 15 and 20 K min^{-1}. The evaluation of the kinetic parameters was performed using Coats-Redfern method. For these kinetic models in the range $0.05 \leq \alpha \leq 0.95$ for decomposition stage of DBBD, the straight lines corresponding to Coats-Redfern method is characterized by correction coefficient values close to unity also values close to the mean isoconversional activation energies [40–42].

The apparent kinetic parameters for the thermal decomposition in nitrogen flow for DBBD and are represented in ln A *versus* E_a (Figs. S6 and S7) for stages I and II, respectively. The evaluation of the invariant kinetic parameters is performed using the super-correction (Eq. 7). The plot of a_β *versus* b_β, obtained for three different heating rates, is a straight line, from which $\ln A_{inv}$ and E_{inv} are determined. The detailed images of the plots for DBBD (Stages I and II) (Figs. S6 and S7) (undersized figure in up-left corner) show the incompatibility of few models among all other conversion function, although its apparent parameters were obtained with high correlation coefficients.

For several groups of apparent activation parameters, obtained by different kinetic models, we tried to establish the best combination ($r \rightarrow 1$), a better resolution in determining the invariant kinetic parameters and the closest value to the mean isoconversional activation energies [41].

For stage I, for AKM – {D1, D2, D3, D4}, the plots of ln A *versus* E_a have highest correlation coefficient from the slope and intercept values a_β and b_β, we calculated (Tables S9 and S10) invariant kinetic parameter E_{inv} = 28.40 kJ mol^{-1} and $\ln A_{inv}$ = 3.90 A min^{-1} are obtained with r = 1.000 and is a true straight line. For these groups, the invariant activation energy is almost equal to the average values of E_a obtained by KAS method (30.36 ± 11.45 kJ mol^{-1}).

For stage II, for AKM – {D1, D3, D4}, the plots of ln A *versus* E_a have highest correlation coefficient from the slope and intercept values a_β and b_β, we calculated invariant kinetic parameter E_{inv} = 105.07 kJ mol^{-1} and $\ln A_{inv}$ = 19.20 A min^{-1} (Tables S11 and S12) are obtained with r = 0.9993. For these groups, the invariant activation energy is almost equal to average values obtained by FWO method (104.28 ± 10.27 kJ mol^{-1}). The rate of decomposition of first stage is faster when compare to second stage due to the energy of activation is higher for stage II.

3.5. Kinetic model determination

The most suitable kinetic model for the decomposition process of stage I is P2. By introducing the derived reaction model $g(\alpha) = (\alpha)^{1/3}$ the following equation is obtained [43]. The plots of $(\alpha)^{1/3}$ against $E_a P(x)/\beta R$ at the different heating rates are shown in Fig. 4.

$$(\alpha)^{1/3} = AE_aP(x)/\beta R \quad \ldots (14)$$

Manikandan *et al.* have investigated kinetics and vapourization of anil in nitrogen atmosphere – non-isothermal condition follows kinetic model P2 [44].

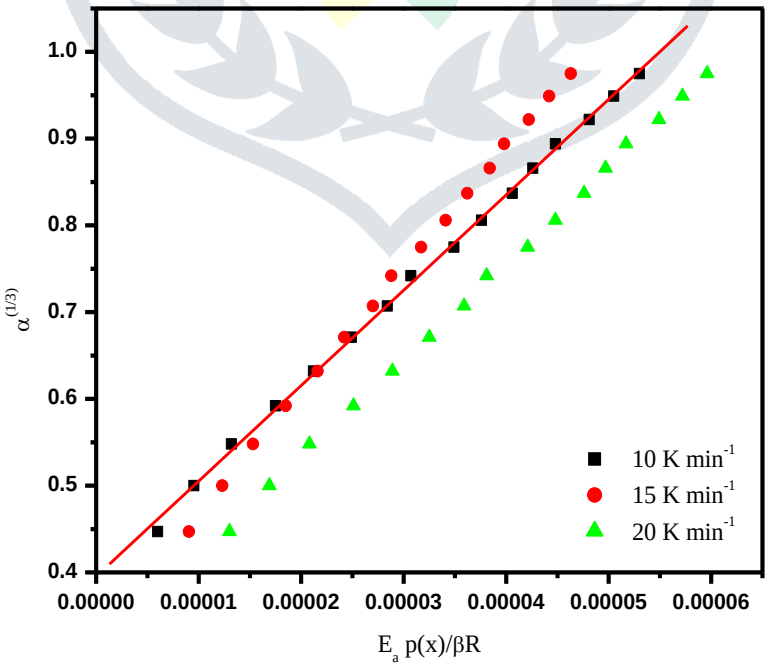

Fig. 4 Plot of $\alpha^{1/3}$against $E_aP(x)/\beta R$ for the decomposition of N^1,N^4-dibenzylidenebenzene-1,4-diamine (DBBD) at different heating rates (β) (Stage I)

The most suitable kinetic model for the decomposition process of DBBD is P3 for stage II. By introducing the derived reaction model $g(\alpha) = (\alpha)^{1/2}$, the following equation is obtained

$$(\alpha)^{1/2} = AE_a P(x)/\beta R \quad \ldots (15)$$

The plots of $(\alpha)^{1/2}$ against $E_a P(x)/\beta R$ at the different heating rates are shown in Fig. 5.

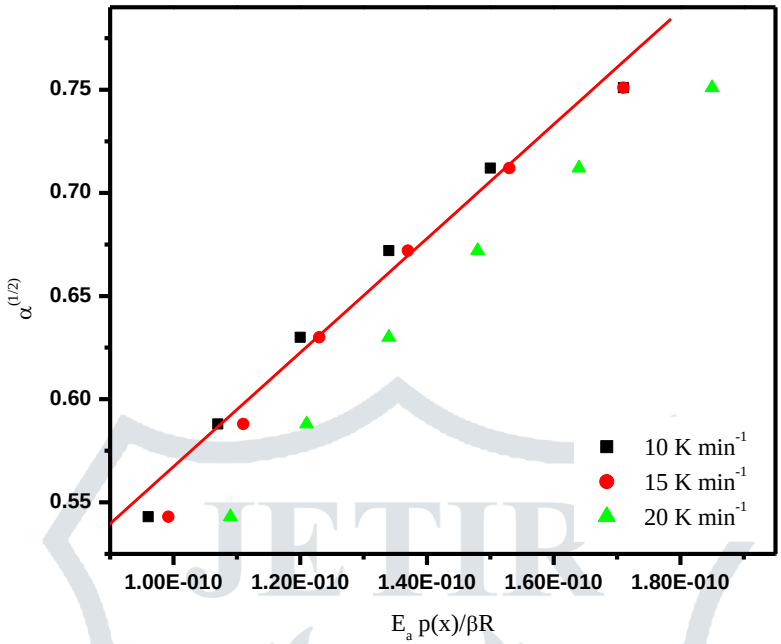

Fig. 5 Plot of $\alpha^{1/2}$ against $E_aP(x)/\beta R$ for the decomposition of N^1,N^4-dibenzylidenebenzene-1,4-diamine (DBBD) at different heating rates (β) (Stage II)

3.6. Thermodynamic parameters

From the DTA curves, the peak temperature for DBBD are 441, 448, 451 K (Stage I) and 637, 644, 650 K (Stage II) at different heating rates at 10, 15 and 20 K min^{-1}. These peak temperatures were used to determine single point kinetic parameters [25]. The obtained E_a values were 97.24 ± 4.03 and 171.83 ± 7.28 kJ mol^{-1} for stages I and II (Table 1), respectively.

Table 1 Values of kinetic and thermodynamic parameters for the thermal decomposition of DBBD in the nitrogen atmosphere

Parameters	Stage I	Stage II
E_a/kJ mol^{-1}	97.24 ± 4.03	171.83 ± 7.28
ln A/A min^{-1}	25.97 ± 7.27	31.70 ± 8.13
$\Delta G^{\neq}$/k $Jmol^{-1}$	111.68	163.91
$\Delta H^{\neq}$/k $Jmol^{-1}$	93.53	166.47
$\Delta S^{\neq}$/$Jmol^{-1}$	–40.62	3.97
r	–0.9991	–0.9991

The thermodynamic parameters, $\Delta S^{\#}$, $\Delta H^{\#}$ and $\Delta G^{\#}$ were determined at the peak temperature T_m in the DTA curves for the corresponding stage [45]. Since the temperature characterizes the higher rate of decomposition and therefore, it is an important parameter. As can be seen from Table 1, the value of $\Delta S^{\#}$ for the compound is negative for stage I. It means that the corresponding activated complex were with lesser degree of arrangement than the initial stage [35]. The positive values of $\Delta H^{\#}$ and $\Delta G^{\#}$ show that they are connected with absorption of heat and are attributed to non-spontaneous process [45,46].

4. CONCLUSION

The compound chosen for this study decomposed into two stages. The decomposition of DBBD followed different kinetic models namely P2 for stage I and P3 for stage II, respectively. Since the activation energy values slightly varied with the conversion level, the average activation energy values were used to interpret decomposition models for each stage. The rate of decomposition of first stage is faster when compared to second stage due to energy of activation is higher for stage II. The free energy changes occurred for the compound is positive values for both decomposition stages, which indicate that the decomposition of studied compound is non-spontaneous process.

ACKNOWLEDGMENTS

The authors thank Head of the Department, CECRI, Alagappa University, Karaikudi, Tamilnadu, India for recorded TG/DTA thermogram.

REFERENCES

[1] Valcarcel, M. and Laque de Castro, M.D. 1994. Flow-through biochemical sensors. Elsevier, Amsterdam.
[2] Spichiger-Keller, U. 1998. Chemical sensors and biosensors for medical and biological applications. Wiley-VCH, Weinheim.
[3] Lawrence, J.F. and Frei, R.W. 1976. Chemical derivatization in chromatography. Elsevier, Amsterdam.
[4] Patai, S. 1970. The chemistry of the carbon-nitrogen double bond. John Wiley & Sons, London.
[5] Metzler, C.M., Cahill, A. and Metzler, D.E. 1980. Journal of the American Chemical Society, 102: 6075–6082.
[6] Clarke, B., Clarke, N., Cunningham, D., Higgins, T., McArdle, P., Cholchuin, M.N. and O'Gara, M. 1998. Journal of Organometallic Chemistry, 559: 55–64.
[7] Pandeya, S.N., Sriram, D., Nath, G. and De Clercq, E. 1999. Pharmaceutica Acta Helvetiae, 74: 11–17.
[8] Pandeya, S.N., Sriram, D., Nath, G. and De Clercq, E. 2000. Arzneimittel Forschung, 50: 55–59.
[9] Singh, W.M. and Dash, B.C. 1988. Pesticides, 22: 33–37.
[10] Kelley, J.L., Linn, J.A., Bankston, D.D., Burchall, C.J., Soroko F.E. and Copper, B.R. 1995. Journal of Medicinal Chemistry, 38: 3676–3679.
[11] Schmid, G.H. 1996. Organic Chemistry. McGraw-Hill, New York, p. 1306.
[12] Zhang, S., Niu, Q., Lan, L. and Li, T. 2017. Sensors and Actuators B, 240: 793–800.
[13] Cheng, L., Tang, J., Luo, H., Jin, X., Dai, F., Yang, J., Qian, Y., Li, X. and Zhou, B. 2010. Bioorganic & Medicinal Chemistry Letters, 20: 2417–2420.
[14] Cozzi, P.G. 2004. Chemical Society Reviews, 33: 410–421.
[15] Ferreira, M.L., Vasconcelos, T.A., Carvalho, E., Lourenco, M., Wardell, S.V., Wardell, J., Ferreira, V. and Souza, M. 2009. Carbohydrate Research, 344: 2042–2047.
[16] Raman, N., Mittu, L., Sakthivel, A. and Pandi, M.S.S. 2009. Journal of the Iranian Chemical Society, 6: 738–748.
[17] Elangovan, N., Kolochi, T. and Sowrirajan, S. 2016. International Journal of Current Research in Chemistry and Pharmaceutical Sciences, 3: 60–65.
[18] Scozzatava, A. and Supuran, C.T. 2000. Bioorganic & Medicinal Chemistry Letters, 10: 1117–1120.
[19] Friedman, H.L. 1964. Journal of Polymer Science C: Polymer Symposia, 6: 183–195.
[20] Flynn, J.H. and Wall, L.A. 1966. Journal of Research of the National Bureau of Standards A, 70: 487–523.
[21] Ozawa, T. 1965. Bulletin of the Chemical Society of Japan, 38: 1881–1886.
[22] Doyle, C.D. 1961. Journal of Applied Polymer Science, 5: 285–292.
[23] Doyle, C.D. 1965. Nature, 207: 290–291.
[24] Doyle, C.D. 1962. Journal of Applied Polymer Science, 6: 639–642.
[25] Kissinger, H.E. 1957. Analytical Chemistry, 29: 1702–1706.
[26] Akahira, T. and Sunose, T. 1971. Joint convention of four electrical institutes. Research Report (Chiba Institute of Technology), Chiba, Vol. 16, pp. 22–31.
[27] Coats, A.W. and Redfern, J.P. 1964. Nature (London), 201: 68–69.
[28] Horowitz, H.H. and Metzger, G.A. 1963. Analytical Chemistry, 35: 1464–1468.
[29] Criado, J.M. and Morales, J. 1976. Thermochimica Acta, 16: 382–387.
[30] Lesnikovich, A.I. and Levchik, S.V. 1985. Journal of Thermal Analysis and Calorimetry, 30: 237–262.
[31] Flynn, J.H. 1997. Thermochimica Acta, 300: 83–92.
[32] Senum, G.I. and Yang, R.T. 1977. Journal of Thermal Analysis and Calorimetry, 11: 445–447.
[33] Kissinger, H.E. 1956. Journal of Research of the National Bureau of Standards, 57: 217–221.
[34] Whelan, D.J., Spear, R.J. and Read, R.W. 1984. Thermochimica Acta, 80: 149–163.
[35] Malek, J. 1989. Thermochimica Acta, 136: 337–346.
[36] Cordes, H.F. 1968. Journal of Physical Chemistry, 72: 2185–2189.
[37] Bamford, C.H. and Tipper, C.F.H. (Eds.). 1980. Reactions in the solid state. Comprehensive chemical kinetics. Vol. 22, Elsevier, Amsterdam.
[38] Vyazovkin, S. and Linert, W. 1995. Chemical Physics, 193: 109–118.
[39] Lesnikovich, A.I. and Levchik, S.V. 1983. Journal of Thermal Analysis and Calorimetry, 27: 89–94.
[40] Vyazovkin, S.V. and Lesnikovich, A.I. 1998. Thermochimica Acta, 128: 297–300.
[41] Budrugeac, P. and Segal, E. 2007. Journal of Thermal Analysis and Calorimetry, 88: 703–707.
[42] Pratap, A., Rao, T.L.S., Lad, K.N. and Dhurandhar, H.D. 2007. Journal of Thermal Analysis and Calorimetry, 89: 399–405.
[43] Malek, J. 1992. Thermochimica Acta, 200: 257–269.
[44] Manikandan, G., Jayabharathi, J., Rajarajan, G. and Thanikachalam, V. 2012. Journal of King Saud University Science, 24: 265–270.
[45] Criado, J.M., Perez-Maqueda, L.A. and Sanchez-Jimenez, P.E. 2005. Journal of Thermal Analysis and Calorimetry, 82: 671–675.
[46] Sokolskii, D.V. and Druz, V.A. 1981. Introduction in theory of heterogeneous catalysis. Vyshaya Shkola, Moscow, Russia.

SUPPLEMENTARY MATERIAL

Table S1 Nonisothermal kinetic data of N^1,N^4-dibenzylidenebenzene-1,4-diamine (DBBD) – Stage I

α	10 K	15 K	20 K	Flynn-Wall-Ozawa method			Kissinger-Akahira-Sunose method			Friedman method	
				E_a (kJ mol^{-1})	ln A (A min^{-1})	-r	E_a (kJ mol^{-1})	ln A (A min^{-1})	-r	E_a (kJ mol^{-1})	-r
0.05	388.06	443.90	499.75	9.5309	0.661167	0.9997	2.7404	-2.9366	0.9827	-	-
0.10	422.58	469.29	504.99	14.1363	1.379599	0.9996	7.2208	-0.9470	0.9995	52.8182	0.9292
0.15	457.10	492.13	518.16	21.1978	2.605143	0.9998	14.2250	1.2572	0.9997	52.6298	0.9920
0.20	479.44	506.86	530.68	27.2601	3.684262	0.9996	20.2963	2.8703	0.9989	52.8873	0.9952
0.25	494.67	518.02	541.01	31.7087	4.454298	0.9977	24.7548	3.9386	0.9955	52.1724	0.9881
0.30	505.84	526.15	549.31	34.9711	5.001433	0.9937	28.0179	4.6691	0.9888	52.4431	0.9626
0.35	515.99	533.26	557.22	37.7489	5.447441	0.9856	30.7827	5.2504	0.9758	52.9820	0.9154
0.40	523.10	539.35	563.14	39.6517	5.736176	0.9828	32.6738	5.6235	0.9718	52.3416	0.9694
0.45	529.19	543.92	568.24	41.0737	5.939829	0.9760	34.0734	5.8833	0.9615	52.6919	0.9003
0.50	534.27	548.49	572.70	42.3315	6.116251	0.9740	35.3162	6.1083	0.9590	52.5381	0.9639
0.55	537.32	551.02	575.37	43.0160	6.207788	0.9714	35.9878	6.2243	0.9552	52.8547	0.9285
0.60	542.39	555.09	579.83	44.0242	6.332525	0.9652	36.9672	6.3817	0.9463	52.9797	0.8946
0.65	545.44	558.13	582.67	44.7759	6.431585	0.9657	37.7090	6.5072	0.9474	52.4510	0.9800
0.70	548.49	560.67	585.45	45.2986	6.486995	0.9622	38.2095	6.5770	0.9424	52.0507	0.8968
0.75	550.52	563.21	587.45	45.9782	6.584138	0.9664	38.8917	6.6998	0.9489	52.3052	0.9940
0.80	552.55	564.73	589.28	46.2619	6.608549	0.9628	39.1571	6.7303	0.9436	52.6952	0.8375
0.85	555.59	567.27	592.11	46.7140	6.648158	0.9590	39.5829	6.7800	0.9382	52.1742	0.8835
0.90	557.63	569.30	594.08	47.1312	6.694838	0.9591	39.9885	6.8389	0.9386	52.0359	0.9666
0.95	559.66	571.33	596.04	47.5633	6.744216	0.9593	40.4098	6.9010	0.9390	52.8536	0.9679
Mean				37.388 ± 11.531			30.368 ± 11.4517			52.550 ±0.3173	

Table S2 Nonisothermal kinetic data of N^1,N^4-dibenzylidenebenzene-1,4-diamine (DBBD) –Stage II

α	10 K	15 K	20 K	Flynn-Wall-Ozawa method			Kissinger-Akahira-Sunose method			Friedman method	
				E_a (kJ mol^{-1})	ln A (A min^{-1})	-r	E_a (kJ mol^{-1})	ln A (A min^{-1})	-r	E_a (kJ mol^{-1})	-r
0.05	568.07	579.45	590.82	80.9136	13.4014	0.9963	75.4714	14.7114	0.9952	-	-
0.10	573.32	584.69	595.05	86.2157	14.3342	0.9982	80.9703	15.7620	0.9977	118.2380	0.9953
0.15	578.13	589.07	599.12	90.6132	15.0865	0.9980	85.5213	16.6036	0.9975	118.2521	0.9983
0.20	582.51	593.22	602.94	94.4078	15.7178	0.9982	89.4443	17.3069	0.9978	118.7303	0.9997
0.25	586.44	596.94	606.46	97.5575	16.2254	0.9982	92.6950	17.8705	0.9978	118.8576	0.9989
0.30	589.94	600.44	609.66	100.1702	16.6312	0.9987	95.3876	18.3203	0.9984	118.5483	0.9997
0.35	592.57	603.06	612.10	102.0016	16.9068	0.9990	97.2718	18.6252	0.9987	118.5178	0.9999
0.40	596.07	606.35	615.42	104.1199	17.2083	0.9986	99.4427	18.9580	0.9983	118.1078	0.9950
0.45	598.69	608.97	617.92	105.6591	17.4207	0.9988	101.0191	19.1924	0.9985	118.3992	1.0000
0.50	601.32	611.59	620.46	107.0599	17.6036	0.9989	102.4496	19.3941	0.9987	118.1018	0.9998
0.55	603.94	614.22	623.01	108.3624	17.7655	0.9990	103.7767	19.5726	0.9988	118.2259	0.9999
0.60	606.56	616.84	625.58	109.5667	17.9068	0.9991	105.0002	19.7282	0.9989	118.3240	0.9997
0.65	609.63	619.69	628.62	110.8324	18.0450	0.9985	106.2801	19.8800	0.9982	118.7957	0.9865
0.70	612.25	622.31	631.23	111.8302	18.1433	0.9985	107.2860	19.9884	0.9982	118.2507	0.9987
0.75	614.44	624.72	633.40	112.7301	18.2352	0.9992	108.1969	20.0898	0.9990	118.9965	0.9922
0.80	617.06	627.56	636.02	113.6334	18.3110	0.9996	109.1040	20.1737	0.9995	118.3896	0.9943
0.85	619.69	630.18	638.68	114.4218	18.3663	0.9996	109.8892	20.2347	0.9995	118.5210	0.9989
0.90	622.75	633.24	641.79	115.2508	18.4129	0.9995	110.7097	20.2861	0.9994	118.5122	0.9989
0.95	625.81	636.53	644.89	116.0611	18.4528	0.9998	111.5113	20.3307	0.9998	118.7372	0.9958
Mean				104.284 ± 10.271			99.548 ± 10.533			118.472 ±0.265	

Table S3 Arrhenius parameters for the non-isothermal decomposition of N^1,N^4-dibenzylidenebenzene-1,4-diamine (DBBD) – Stage I using the Coats-Redfern method at heating rate of 10 K min^{-1}

Model	ln A (A min^{-1})	E_a (kJ mol^{-1})	-r
P2	7.5676	-2.0468	0.9359
P3	2.4176	-4.2460	0.8051
F1	31.7755	5.0288	0.9098
F2	43.9529	8.7422	0.8351
F3	58.9000	13.1747	0.7745
D1	62.0551	18.8839	0.9784
D2	58.6930	10.1925	0.9627
D3	64.7538	10.4755	0.9443
D4	64.4700	10.1076	0.9521
A2	11.9619	-0.3525	0.8607
A3	5.2814	-2.6548	0.7588
A4	2.0551	-4.3161	0.5204
R2	26.9707	2.8243	0.9424
R3	25.6117	2.6673	0.9512

Table S4 Arrhenius parameters for the non-isothermal decomposition of N^1,N^4-dibenzylidenebenzene-1,4-diamine (DBBD) – Stage I using the Coats-Redfern method at heating rate of 15 K min^{-1}

Model	ln A (A min^{-1})	E_a (kJ mol^{-1})	-r
P2	15.8450	0.8074	0.9846
P3	7.7268	-1.5868	0.9743
F1	54.7365	10.7572	0.9492
F2	75.1202	16.1917	0.8849
F3	100.2240	22.7608	0.8279
D1	98.4180	27.3181	0.9918
D2	96.7928	19.0223	0.9835
D3	106.8823	20.1542	0.9703
D4	106.2536	19.7098	0.9760
A2	23.1378	3.0321	0.9327
A3	12.4772	0.0990	0.9075
A4	7.3385	-1.5483	0.8606
R2	46.7417	7.8874	0.9736
R3	44.4888	7.5447	0.9796

Table S5 Arrhenius parameters for the non-isothermal decomposition of N^1,N^4-dibenzylidenebenzene-1,4-diamine (DBBD) – Stage I using the Coats-Redfern method at heating rate of 20 K min^{-1}

Model	ln A (A min^{-1})	E_a (kJ mol^{-1})	-r
P2	23.6570	2.8981	0.9814
P3	12.7146	0.0850	0.9716
F1	77.8377	15.6494	0.9735
F2	108.0443	22.9771	0.9280
F3	145.3844	31.9022	0.8809
D1	132.9946	34.2220	0.9902
D2	133.6586	26.3735	0.9888
D3	148.5620	28.4330	0.9843
D4	148.3273	28.0844	0.9943
A2	34.3664	5.7699	0.9668
A3	19.6734	2.1493	0.9566
A4	12.6308	0.2381	0.9423
R2	66.0648	12.0513	0.9851
R3	62.7603	11.5061	0.9868

Table S6 Arrhenius parameters for the non-isothermal decomposition of N^1,N^4-dibenzylidenebenzene-1,4-diamine (DBBD) – Stage II using the Coats-Redfern method at heating rate of 10 K min^{-1}

Model	ln A (A min^{-1})	E_a (kJ mol^{-1})	-r
P2	58.1549	9.5678	0.9603
P3	35.4160	4.6641	0.9527
P4	24.1146	2.0891	0.9429
F1	177.4161	34.5521	0.9938
F2	251.7785	50.3437	0.9870
F3	344.6534	69.9121	0.9641
D1	277.6890	61.4377	0.9707
D2	289.8105	55.8054	0.9793
D3	325.6245	61.8652	0.9893
D4	320.9136	60.6087	0.9855
A2	83.7452	15.2685	0.9930
A3	52.0627	8.5248	0.9914
A4	36.9097	5.1828	0.9909
R2	149.0279	27.7728	0.9840

R3	141.1643	26.3556	0.9790

Table S7 Arrhenius parameters for the non-isothermal decomposition of N^1,N^4-dibenzylidenebenzene-1,4-diamine (DBBD) – Stage II using the Coats-Redfern method at heating rate of 15 K min^{-1}

Model	**ln A (A min^{-1})**	**E_a (kJ mol^{-1})**	**-r**
P2	61.2135	10.3912	0.9557
P3	37.3921	5.3559	0.9477
P4	25.5527	2.7177	0.9375
F1	186.7075	36.1907	0.9928
F2	265.5827	52.6166	0.9889
F3	364.1619	72.9894	0.9680
D1	290.9376	63.5339	0.9670
D2	304.1506	58.0470	0.9762
D3	342.0739	64.3995	0.9873
D4	336.8326	63.0539	0.9826
A2	88.2997	16.2998	0.9918
A3	55.0128	9.3518	0.9901
A4	39.0958	5.9141	0.9895
R2	156.6404	29.1776	0.9813
R3	148.3195	27.6971	0.9759

Table S8 Arrhenius parameters for the non-isothermal decomposition of N^1,N^4-dibenzylidenebenzene-1,4-diamine (DBBD) – Stage II using the Coats-Redfern method at heating rate of 20 K min^{-1}

Model	**ln A (A min^{-1})**	**E_a (kJ mol^{-1})**	**-r**
P2	66.0186	11.4785	0.9494
P3	40.5383	6.1961	0.9410
P4	27.8745	3.4385	0.9304
F1	200.9179	38.7348	0.9900
F2	286.3772	56.2105	0.9892
F3	393.2413	77.9050	0.9703
D1	311.2658	66.9804	0.9614
D2	326.1959	61.7654	0.9715
D3	367.2486	68.6156	0.9837
D4	361.5472	67.1958	0.9788
A2	95.3241	17.7398	0.9889
A3	59.6008	10.4196	0.9867
A4	42.5273	6.8079	0.9859
R2	168.3727	31.3274	0.9769
R3	159.3718	29.7388	0.9710

Table S9 The compensation effect parameters for several combination of kinetic models for N^1,N^4-dibenzylidenebenzene-1,4-diamine (DBBD) – Stage I

β (Kmin^{-1})	AKM			AKM-{D1}		
	a_β (A min^{-1})	b_β (mol J^{-1})	r	a_β (A min^{-1})	b_β (mol J^{-1})	r
10	-4.2415	0.2741	0.9510	-3.8995	0.2479	0.9789
15	-3.0103	0.2440	0.9744	-2.6780	0.2288	0.9911
20	-2.3596	0.2266	0.9838	-2.0732	0.2164	0.9948
β (K min^{-1})	AKM-{D1,D3}			AKM-{D1,D2,D4}		
	a_β (A min^{-1})	b_β (mol J^{-1})	r	a_β (A min^{-1})	b_β (mol J^{-1})	r
10	-4.0477	0.2581	0.9810	-4.3564	0.2759	0.9906
15	-2.8405	0.2348	0.9918	-3.1743	0.2473	0.9960
20	-2.2385	0.2207	0.9953	-2.5762	0.2295	0.9977
β (K min^{-1})	AKM-{D1,D3,D4,D2}			AKM-{D1,D3,D4,D2,R2}		
	a_β (A min^{-1})	b_β (mol J^{-1})	r	a_β (A min^{-1})	b_β (mol J^{-1})	r
10	-4.6162	0.3001	0.9974	-4.5680	0.3013	0.9982
15	-3.4432	0.2588	0.9988	-3.3872	0.2595	0.9994
20	-2.8239	0.2370	0.9993	-2.7632	0.2374	0.9996
β (K min^{-1})	AKM-{D1,D3,D4,D2,R2,A2}			AKM-{D1,D3,D4,D2,R2,A2,A3}		
	a_β (A min^{-1})	b_β (mol J^{-1})	r	a_β (A min^{-1})	b_β (mol J^{-1})	r
10	-4.6875	0.3032	0.9989	-4.8200	0.3061	0.9992
15	-3.4708	0.2603	0.9995	-3.5733	0.2616	0.9996
20	-2.8388	0.2379	0.9997	-2.9366	0.2388	0.9997
β (K min^{-1})	AKM-{D1,D3,D4,D2,R2,A2,A3,P2}			AKM-{D1,D3,D4,D2,R2,A2,A3,P2,R3}		
	a_β (A min^{-1})	b_β (mol J^{-1})	r	a_β (A min^{-1})	b_β (mol J^{-1})	r
10	-4.9935	0.3097	0.9997	-4.9328	0.3094	0.9999
15	-3.6664	0.2628	0.9996	-3.5544	0.2624	0.9999
20	-3.0105	0.2394	0.9997	-2.8855	0.2391	0.9999

Table S10 IKP for several combination of kinetic models for N^1,N^4-dibenzylidenebenzene-1,4-diamine (DBBD) – Stage I

Kinetic model	E_{inv} (kJ mol^{-1})	ln A_{inv} (A min^{-1})	r
AKM	39.7606	6.6661	0.9997
AKM - {D1}	58.4838	10.6281	0.9975
AKM - {D1,D3}	48.7185	8.5462	0.9987
AKM - {D1,D3,D4}	38.6450	6.3270	0.9985
AKM - {D1,D3,D4,D2}	28.4038	3.9077	1.0000
AKM - {D1,D3,D4,D2,R2}	28.2447	3.9421	1.0000
AKM - {D1,D3,D4,D2,R2,A2}	28.3175	3.8988	1.0000
AKM - {D1,D3,D4,D2,R2,A2,A3}	27.9893	3.7478	1.0000
AKM - {D1,D3,D4,D2,R2,A2,A3,P2}	28.2203	3.7472	1.0000
AKM - {D1,D3,D4,D2,R2,A2,A3,P2,R3}	29.1520	4.0889	0.9999

Table S11 The compensation effect parameters for several combination of kinetic models for N^1,N^4-dibenzylidenebenzene-1,4-diamine (DBBD) – Stage II

β ($K min^{-1}$)	AKM			AKM-{D1}		
	a_β ($A min^{-1}$)	b_β ($mol J^{-1}$)	r	a_β ($A min^{-1}$)	b_β ($mol J^{-1}$)	r
10	-2.3426	0.2059	0.9961	-2.1672	0.202	0.9988
15	-1.9182	0.2022	0.9963	-1.7483	0.1985	0.9989
20	-1.5795	0.1989	0.9966	-1.4161	0.1955	0.9990
β ($K min^{-1}$)	AKM-{D1,D3}			AKM-{D1,D3,D4}		
	a_β ($A min^{-1}$)	b_β ($mol J^{-1}$)	r	a_β ($A min^{-1}$)	b_β ($mol J^{-1}$)	r
10	-2.3183	0.2039	0.9989	-2.594	0.2074	0.9995
15	-1.8991	0.2003	0.9990	-2.1721	0.2036	0.9995
20	-1.5667	0.1971	0.9991	-1.8383	0.2002	0.9996
β ($K min^{-1}$)	AKM-{D1,D3,D4,D2}			AKM-{D1,D3,D4,D2,A2}		
	a_β ($A min^{-1}$)	b_β ($mol J^{-1}$)	r	a_β ($A min^{-1}$)	b_β ($mol J^{-1}$)	r
10	-2.7742	0.2102	0.9998	-2.8411	0.2104	0.9998
15	-2.3489	0.2062	0.9998	-2.4155	0.2064	0.9998
20	-2.0119	0.2026	0.9998	-2.0782	0.2028	0.9998
β ($K min^{-1}$)	AKM-{D1,D3,D4,D2,A2,R2}			AKM-{D1,D3,D4,D2,A2,R2,R3}		
	a_β ($A min^{-1}$)	b_β ($mol J^{-1}$)	r	a_β ($A min^{-1}$)	b_β ($mol J^{-1}$)	r
10	-2.7803	0.2105	0.9999	-2.7194	0.2107	0.9999
15	-2.3544	0.2066	0.9999	-2.2932	0.2067	0.9999
20	-2.0166	0.2029	0.9999	-1.9548	0.203	0.9999

Table S12 IKP for several combination of kinetic models for N^1,N^4-dibenzylidenebenzene-1,4-diamine (DBBD) – Stage II

Kinetic model	E_{inv} ($kJ mol^{-1}$)	ln A_{inv} ($A min^{-1}$)	r
AKM	109.128	20.133	0.9995
AKM - {D1}	115.667	21.202	0.9997
AKM - {D1,D3}	110.652	20.250	0.9994
AKM - {D1,D3,D4}	105.076	19.206	0.9993
AKM - {D1,D3,D4,D2}	100.413	18.340	0.9993
AKM - {D1,D3,D4,D2,A2}	100.492	18.310	0.9993
AKM - {D1,D3,D4,D2,A2,R2}	100.565	18.399	0.9986
AKM - {D1,D3,D4,D2,A2,R2,R3}	99.396	18.232	0.9990

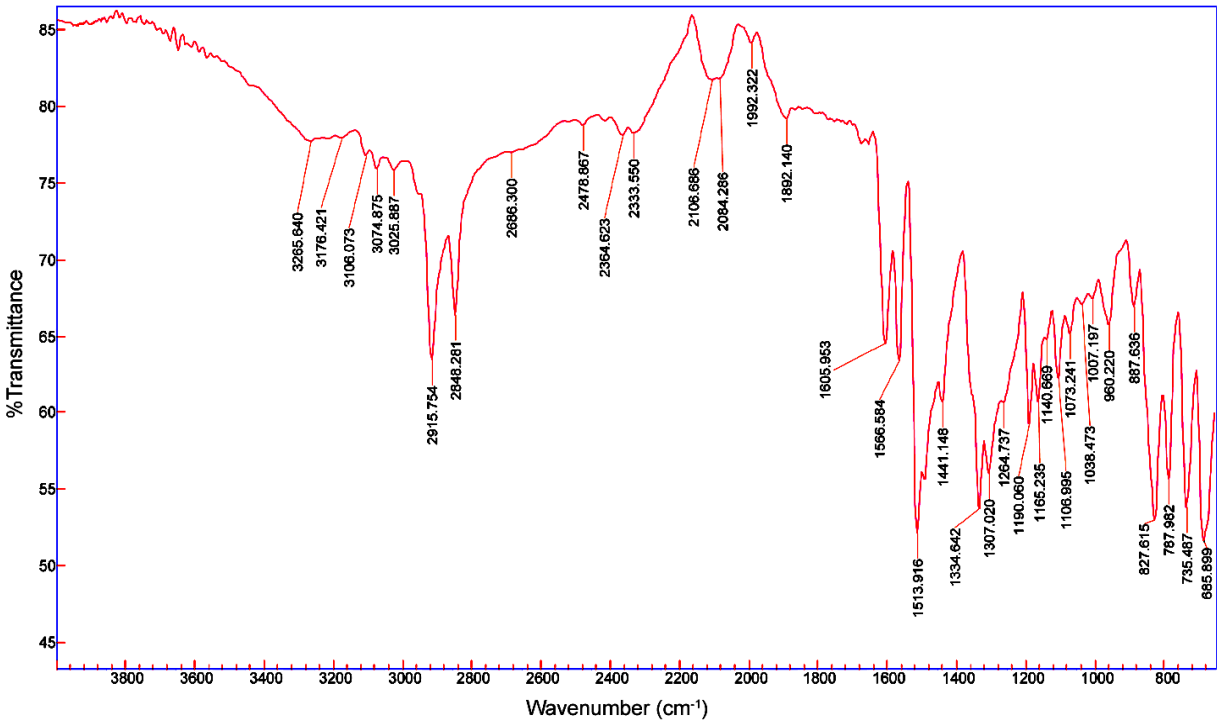

Fig. S1 FT-IR spectrum of N^1,N^4-dibenzylidenebenzene-1,4-diamine (DBBD)

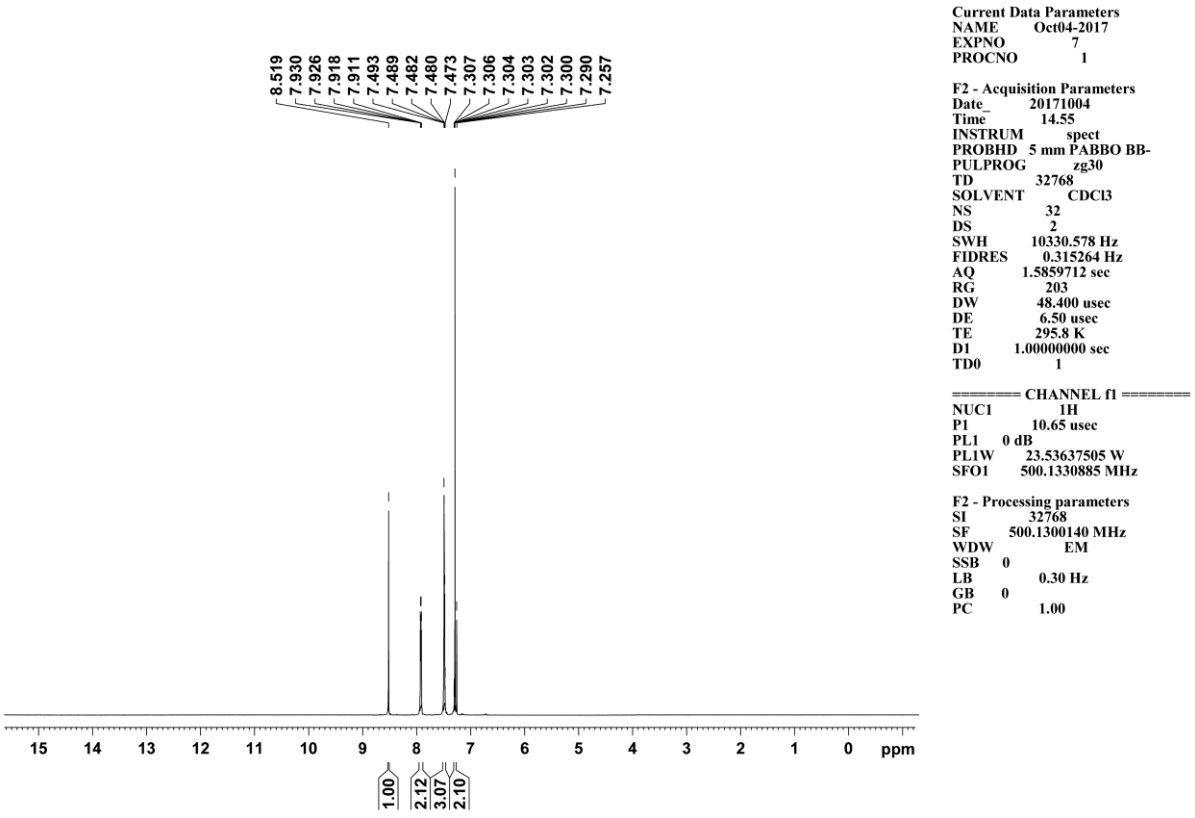

Fig. S2 ^{1}H NMR spectrum of N^1,N^4-dibenzylidenebenzene-1,4-diamine (DBBD)

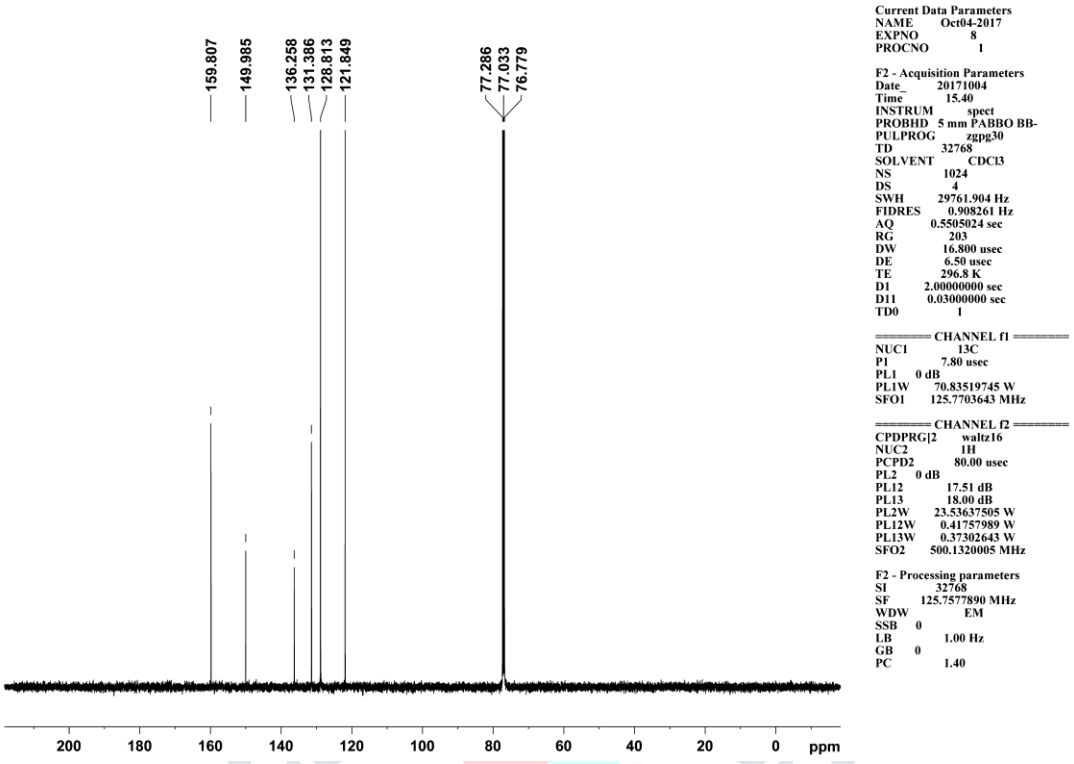

Fig. S3 ^{13}C NMR spectrum of N^1,N^4-dibenzylidenebenzene-1,4-diamine (DBBD)

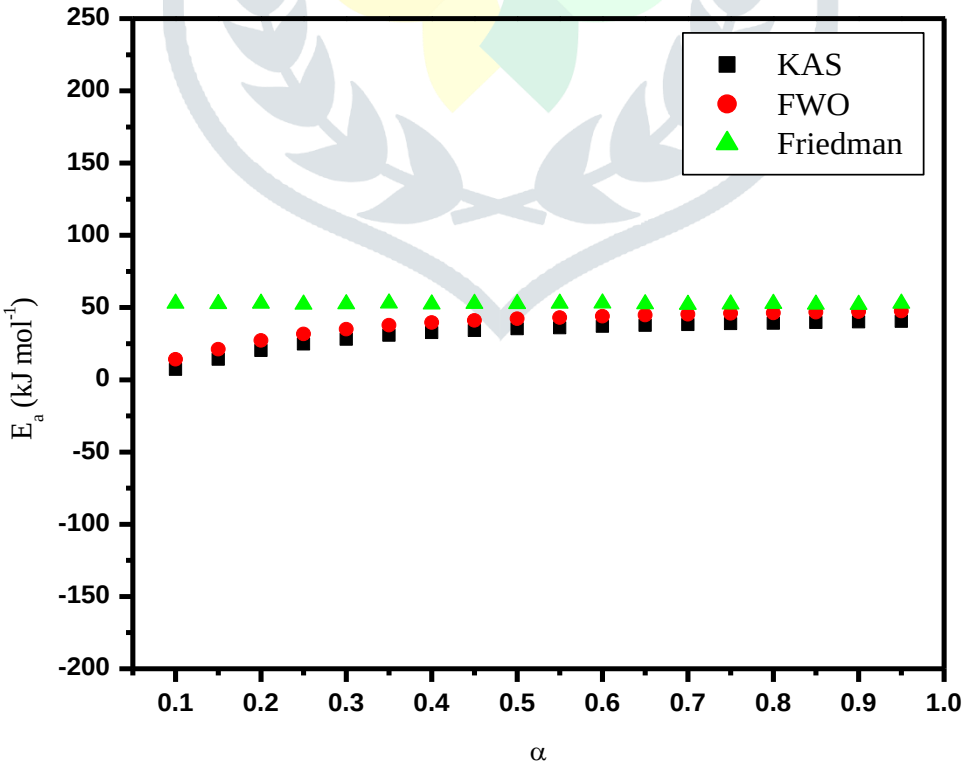

Fig. S4 Plot of α *versus* E_a of N^1,N^4-dibenzylidenebenzene-1,4-diamine (DBBD) – Stage I

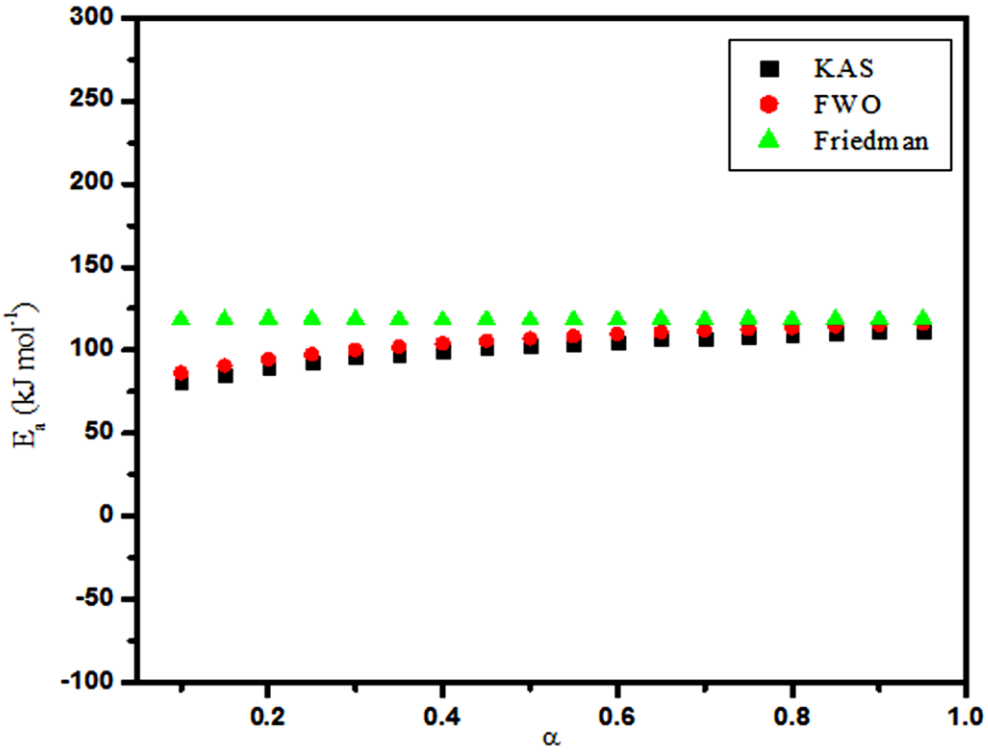

Fig. S5 Plot of α *versus* E_a of N^1,N^4-dibenzylidenebenzene-1,4-diamine (DBBD) – Stage II

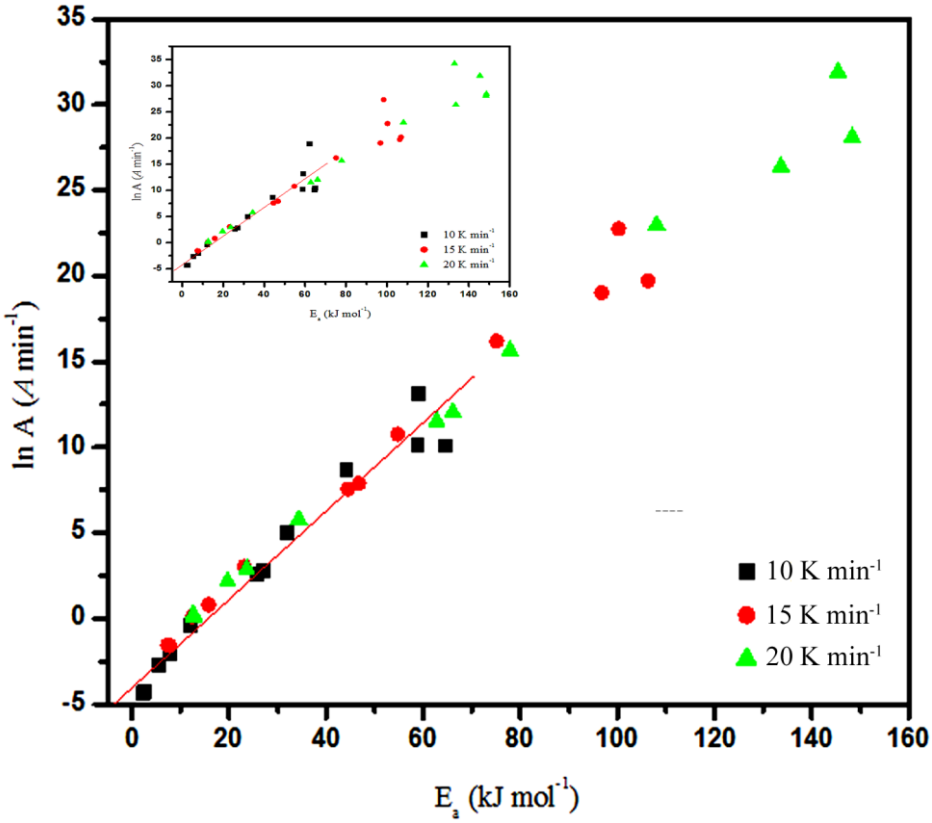

Fig. S6 Dependency of frequency factor on extent of conversion determined using the Coats-Redfern technique for N^1,N^4-dibenzylidenebenzene-1,4-diamine (DBBD) – Stage I at 10, 15 and 20 K min^{-1}

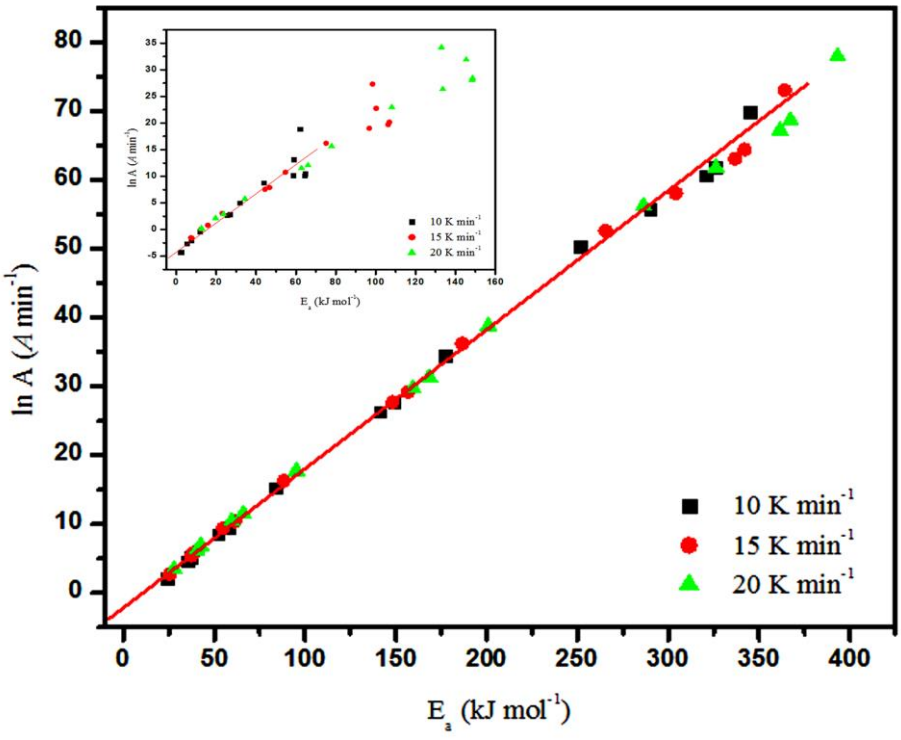

Fig. S7 Dependency of frequency factor on extent of conversion determined using the Coats-Redfern method for N^1,N^4-dibenzylidenebenzene-1,4-diamine (DBBD) – Stage II at 10, 15 and 20 K min^{-1}